Bitlis Eren Üniversitesi Fen Bilimleri Dergisi
BİTLİS EREN UNIVERSITY JOURNAL OF SCIENCE
ISSN: 2147-3129/e-ISSN: 2147-3188
VOLUME: 13 NO: 4 PAGE: 1216-1232 YEAR: 2024
DOI: 10.17798/bitlisfen.1542941

A Novel Approach for Arrhythmia Classification Using CI- 1D-LBP with LSTM, 1D-CNN and GRU Models

Hazret TEKİN[1*], Yılmaz KAYA[2]

[1] *Batman University, Department of Electrical and Electronics Engineering, Batman, Türkiye*
[2] *Batman University, Department of Computer Engineering, Batman, Türkiye*
(ORCID: 0000-0002-9379-721X) (ORCID: 0000-0001-5167-1101)

Keywords: ECG, Center-Independent One-Dimensional Local Binary Pattern (CI-1D-LBP), 1D-CNN, LSTM, GRU.

Abstract

Atrial arrhythmias (ARR) are known as the most encountered cardiac disorders in today's world that have direct or indirect detrimental effect on human health. Therefore, Computer-Assisted Diagnosis (CAD) systems are instrumental in the early detection and diagnosis of diseases, serving a pivotal role in the initial assessment and identification process. In this study, ECG data belonging to four different types of arrhythmias, namely ventricular beat (VB), supraventricular beat (SVB), fusion beat (FB), and an unidentified arrhythmic beat (UB), as well as ECG data showing normal sinus rhythm (NSR) of healthy individuals were classified. The ECG data were sourced from the MIT-BIH database. The Center-Independent 1-Dimensional Local Binary Pattern (CI-1D-LBP), originated from the local binary pattern (LBP) method, proposed as a new approach for deriving the essential features needed for the classification of ECG signals. With this new approach, histograms are generated from the signals, and these histogram data are used as input for classification in 1D-CNN, LSTM, and GRU deep learning methods. The CI-1D-LBP+GRU methodology exhibited superior efficacy in classifying the five-labeled dataset (VB-SVB-FB-UB-NSR) relative to the other applied methods, attaining an impressive accuracy rate of 98.59%.

1. Introduction

The heart works regularly with a heartbeat (pulse) of 60-100 beats per minute, but it may experience arrhythmia because of the disruption of this natural working cycle [1]. Arrhythmia, also known as cardiac rhythm disorder, is caused by the irregularity of heartbeats. Upon the manifestation of these arrhythmias, the heart may present with tachycardia, denoting an abnormally rapid heartbeat; bradycardia, indicating an unusually slow heartbeat; or an irregular rhythm. [2]. Arrhythmias, which are usually seen in people with chronic heart conditions, can also occur in individuals with no pre-existing heart conditions. Therefore, examinations are performed taking into consideration how the arrhythmia is and whether there is any heart disease causing this arrhythmia in patients. Although some arrhythmias may seem harmless at times, some of them can be serious enough to cause life-threatening situations. For example, during an arrhythmia, the heart might struggle to supply sufficient blood to the body, causing symptoms such as shortness of breath, fainting, loss of consciousness, or even sudden death [3].

The most encountered types of arrhythmias in the medical world are ventricular tachycardia (VT), supraventricular tachycardia (SVT), and fusion arrhythmias that arise from the combination of these two arrhythmias [4]. In ventricular tachycardia, the heart rate can increase up to 200-250 beats per minute [5]. As a result of this rapid beating of the heart, the ventricles, which are known as the main pumps that allow blood to circulate throughout the body, may not fill with enough blood, leading to serious health problems [5]. Supraventricular tachycardia is one of

*Corresponding author: hazrettekin@sirnak.edu.tr
Received: 03.09.2024, Accepted: 02.10.2024

the most common types of arrhythmias in infancy and childhood [6]. Especially in infancy, it can manifest itself with symptoms such as restlessness, weakness, and loss of appetite. In children, chest pain and palpitations are among the most prominent complaints, and fainting may occur, albeit rarely [6]. The simultaneous stimulation of the ventricle by both supraventricular and ventricular effects is called a fusion beat or rhythm [7]. Fusion beat arises from the chance encounter of supraventricular and ventricular stimulation in the ventricle [8].

Timely diagnosis of cardiac conditions, such as arrhythmias, coupled with the swift and effective implementation of suitable treatment modalities, mitigates the health risks associated with these disorders. ECG signals, acquired from biomedical electrodes meticulously located at specific anatomical sites, play an indispensable role in the early diagnosis and strategic management of cardiovascular disorders. ECG is a time-resolved signal that meticulously encodes the cardiac electrical activity throughout its cyclical operational phases [9]. The morphological and quantitative characteristics of ECG signals can elucidate intrinsic pathologies, such as arrhythmias, by revealing subtle symptomatic indicators [10]. Substantial quantities of ECG data are procured from an array of modalities, including stationary and mobile ECG devices, holter monitors, [11]. It is essential to establish sophisticated algorithms for the analysis of ECG signals derived from these diverse recording modalities. Prompt and precise diagnosis of cardiac conditions, such as arrhythmias, is critical for enabling swift and effective therapeutic interventions. Therefore, the development of computer-based new technologies is necessary.

The complex and dynamic nature of ECG signals and their susceptibility to noise require a careful selection of signal analysis methods that can provide optimal results in terms of performance [12]. Consequently, it is imperative to advance the development of robust and practical methodologies for signal analysis, feature derivation, and categorization techniques, which can be seamlessly incorporated into Computer-Aided Diagnosis models. The aim of these diagnostic algorithms is to provide the most accurate and fast results while keeping the computational cost and complexity at the lowest level.

In this study, ECG data belonging to four different arrhythmia types, namely ventricular beats (VB), supraventricular tachycardia (SVT), fusion beats (FB), and an unidentified beat (UB), as well as ECG data showing normal sinus rhythm (NSR), were classified.

The data were sourced from the MIT-BIH Arrhythmia Database. In the context of this study, the novel locally binary pattern-based (LBP) Center-Independent 1D-LBP (CI-1D-LBP) methodology was employed to extract the crucial features necessary for the categorization of ECG signals. The CI-1D-LBP method employs a nuanced approach, utilizing binary data derived from the comparison of each of nine discrete points within a window function applied along the ECG signal's length, relative to their neighboring counterparts. Using this method, signal histograms with values ranging from 0 to 255 was generated, and these histogram data were fed as input data to 1D-CNN, LSTM, and GRU deep learning methods. Each deep learning method's hyperparameters were optimized, and their performance results were compared with each other. The proposed method was tested for algorithmic robustness and accuracy performance using ECG datasets (VB-SVB-FB-UB-NSR). In addition, the proposed method was tested on ECG data with different signal lengths obtained as a result of preprocessing steps in the dataset to evaluate its classification performance rates. This allowed us to observe the effect of the length of ECG data on classification performance. When the average accuracy percentages in the application are examined, it is observed that the hybrid CI-1D-LBP+GRU method performs the best in all applications.

Reviewing the literature on the detection of arrhythmia and other cardiac conditions through ECG analysis, it is evident that the process involves a three-stage procedure at its core. During the preliminary stage, ECG signals are purified from noise and other signals caused by hardware effects and external factors by using various filter algorithms. The second stage involves using various mathematical and statistical feature extraction algorithms to determine the features that will characterize the signal and be used for signal classification in the subsequent stage. In the third stage of the process, the features derived from the signal are utilized for classification using suitable machine learning methods with optimized parameters, and the performance is evaluated accordingly. The main aim and motivation of all these processing stages are to achieve high accuracy for the created model while minimizing computational costs.

Thanapatay and colleagues used a hybrid model to classify NSR and four type of arrhythmias. DWT and PCA were employed to derive features from the ECG signal, while SVM were utilized in the subsequent classification phase. The experiments were conducted on 45,686 beats and a reported precision rate of 97.6367% was achieved.[13].

Karpagachelvi and colleagues aimed to classify six different types of heartbeats. They utilized a total of 40,916 beats and applied Discrete Wavelet Transform for extracting features. As classifiers, they employed SVM and ELM and achieved the highest performance of 90.52% using the PSO-SVM classifier [14].

Vijayavanan and colleagues used the morphological attributes of the ECG waveform to extract features. They performed performance analyses using Probabilistic Neural Networks (PNN) in the classification stage. They used Discrete Wavelet Transform (DWT) in the preprocessing stage. They took training periods of 5, 10, 15, and 20 minutes. Approximately 150 records from each category were used for training and 50 records for testing. They found the accuracy of the system to be 96.5% [15].

In their study, Hadiyoso and Rizal employed the Hjorth Descriptor High-Level Complexity to extract features of the ECG signal. The test data consisted of three types of ECG signals: NSR, ARR and Congestive Heart Failure. KNN and MLP (Multilayer Perceptron) were used to classify the features of the signal. By using this method, both MLP and KNN achieved 94% accuracy [16].

Gutiérrez et al. categorized eight distinct types of ECG recordings. They first applied bandpass filtering to the signal and then used Quadratic (2nd order) Wavelet Transform for feature extraction. Probabilistic Neural Networks were used for classification. The overall classification rate varied between 92.746% and 100% [17].

Wu et al. introduced a new approach derived from DIA and YOK for learning ECG arrhythmia features. Gaussian-Bernoulli and Bernoulli-Bernoulli were used to extract the features of ECG data. To enhance the efficacy of the network, a fine-tuning process using backpropagation was performed by appending a softmax regression layer to the hidden representation layer designed for supervised classification. Experimental results showed that the proposed approach achieved successful performance with 99.5% accuracy [18].

Lynn and colleagues proposed the Bi-GRU (Bidirectional Gated Recurrent Units) method as a recurrent neural network (RNN) structure for detecting different types of arrhythmias. The proposed method was compared to LSTM. It was found that the Bi-GRU model, which performed better than LSTM, had an accuracy percentage of 98.55% [19].

Acharya et al. introduced an 11-layer CNN model for the diagnosis of congestive heart failure (CHF). CNN model streamlines the preparation of ECG signals and obviates the necessity for intricate mathematical algorithms in feature extraction This model also reduces the software processing load. The proposed CNN model achieved a high success rate of 98.97% [20].

Han et al. proposed a hybrid method for arrhythmia detection that combines LSTM and 1D-CNN. The proposed architecture was compared to 1D-CNN and Multi-Layer Perceptron (MLP). The accuracy rates were measured as 92.03%, 90.98%, and 86.15% for the hybrid LSTM-1D-CNN, 1D-CNN, and MLP, respectively [21].

Darmawahyuni and colleagues classified ECG data from patients with congestive heart failure (CHF) and healthy individuals. Initially, they employed the Discrete Wavelet Transform to isolate ECG signals from noise. Subsequently, they segmented denoised ECG signals to enhance classification accuracy. Ultimately, the RNN-LSTM architecture was utilized as a deep learning technique for further analysis. The results demonstrated that the proposed method attained accuracy rate surpassing 99% [22].

Zheng et al. applied a pioneering technique, named as Singular Value Decomposition (SVD), for extracting features from ECG signals. CNN and SVM machine learning methods are employed for classification. Optimal average accuracy for both CNN and SVM models was attained when only 3 singular values were selected, with accuracy rates surpassing 96% [23].

In their study, Cinar and Tuncer proposed a novel hybrid deep learning approach for the classification of ECG signals from patients with congestive heart failure, cardiac arrhythmias, and healthy individuals. The presented hybrid AlexNet-SVM model was utilized to classify ECG signals and its performance was benchmarked against other machine learning techniques, including SVM, KNN, and LSTM. Results revealed that SVM achieved an accuracy of 68.75%, KNN attained 65.63%, and LSTM reached 90%. In contrast, the hybrid AlexNet-SVM model, which utilized spectrogram images derived from ECG signals, achieved a remarkable accuracy rate of 96.77% [24].

Mohonta and colleagues introduced an advanced 2D-CNN framework augmented with CWT for the classification of five distinct arrhythmic signal types. This 2D-CNN-based model was adeptly applied to the classification of brief ECG segments (0.225 seconds) utilizing scalograms derived from the continuous wavelet transform. The proposed methodology achieved outstanding performance metrics, with average sensitivity, specificity, and

accuracy rates of 98.87%, 99.85%, and 99.65%, respectively [25].

Madan et al. proposed a hybrid deep learning model for classifying ECG data associated with atrial fibrillation (ARR), congestive heart failure (CHF), and normal sinus rhythm (NSR). They transformed ECG signals into scalogram images to automate noise filtering and feature extraction. The classification was performed using a hybrid CNN-LSTM model, achieving accuracy rates between 98.7% and 99% [26].

Panganiban et al. developed a CNN-based application for arrhythmia classification using spectrogram images of ECG signals. They utilized Google's Inception V3 model to retrain the final layer for this task, classifying ECG datasets into two labeled classes and five labeled classes for training and testing. Their method achieved significant accuracy rates of 98.73% for two-class classification and 97.33% for five-class classification [27].

Salem et al. proposed a method for analyzing and classifying four types of ECG arrhythmias using spectrograms generated from ECG signals via Short-Time Fourier Transform (STFT). These spectrogram images served as input for a hybrid deep learning model that combined DenseNET with SVM, achieving an accuracy of 97.23%. [28]

Rahul and Sharma proposed a hybrid model consisting of 1-D CNN and Bi-LSTM algorithms for the detection of three different types of arrhythmias. A hybrid model composed of stationary wavelet transforms (SWT) and Savitzky-Golay (SG) median filters, which was proposed as a new method for preprocessing ECG data, was used in the preprocessing stage. It was found that the proposed hybrid 1-D CNN-Bi-LSTM classification model had an accuracy rate of 99.44% [29].

2. Material and Method

2.1. Dataset

To test the proposed approach, ECG data for four different types of arrhythmias, including ventricular beats (VB), supraventricular beats (SVB), fusion beats (FB), and an unspecified beat type (UB), as well as ECG data for normal sinus rhythm (NSR) from healthy individuals, were obtained from the MIT-BIH database [30], [31]. The dataset comprises a total of 113,382 ECG recordings, each comprising 187 samples, including 90,589 recordings of normal sinus rhythm (NSR), 7,236 recordings of ventricular tachycardia (VB), 5,179 recordings of supraventricular tachycardia (SVB), 2,339 recordings of fusion beats (FB), and 8,039 recordings of an unidentified beat type (UB). The sampling frequency of the ECG data is given as 125 Hz. The ECG graphs for NSR, VB, SVB, FB, and UB heartbeats are shown in the Figure 1.

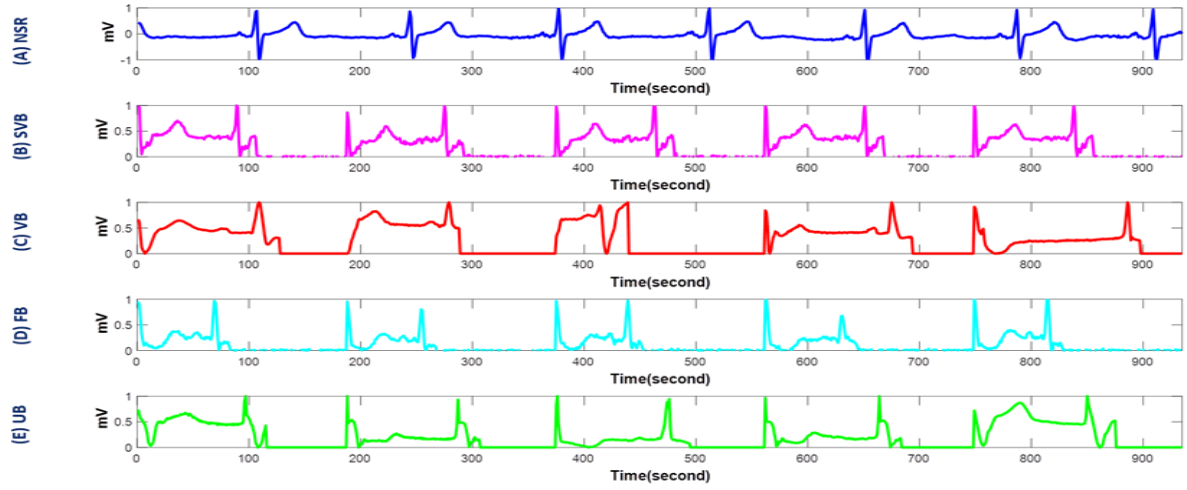

Figure 1. ECG sample signals for (A) NSR, (B) SVB, (C) VB (D) FB, (E) UB

2.2. Proposed Arrhythmia Diagnosis System

The suggested method for extracting features and classifying ECG signals to identify the type of arrhythmia involves four stages as illustrated in Figure 2. Each stage includes a brief explanation of the operations carried out.

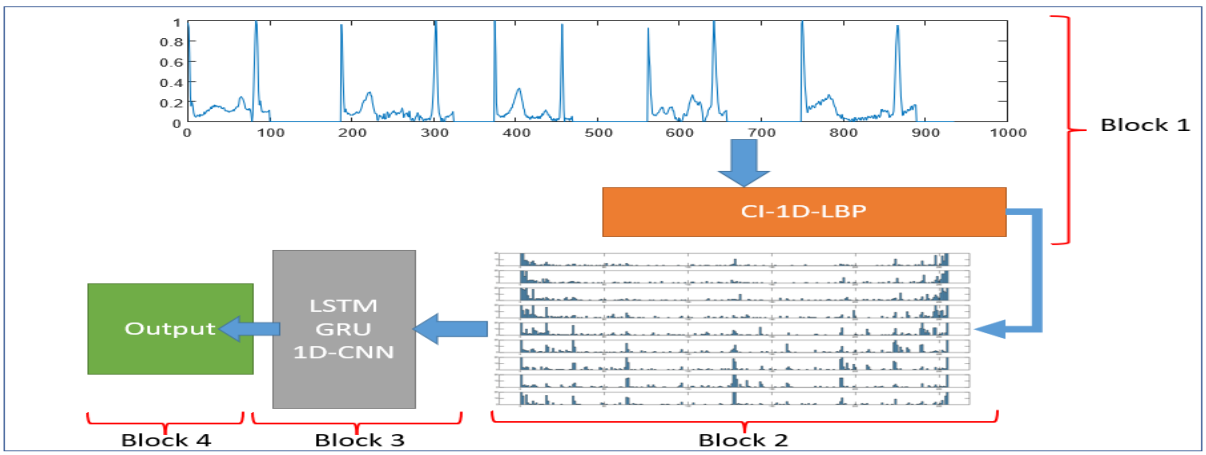

Figure 2. The flow diagram of the proposed arrhythmia classification system

Block 1: In this phase, the CI-1D-LBP method was employed to every individual ECG signal sample within the dataset, acting as a signal transformation procedure. Upon feeding a signal into the CI-1D-LBP method, nine distinct signals are generated as output, where the values of the produced signals exhibit variations between 0 and 255. Figure 3 shows nine different signals obtained by applying the CI-1D-LBP method to an example ECG signal.

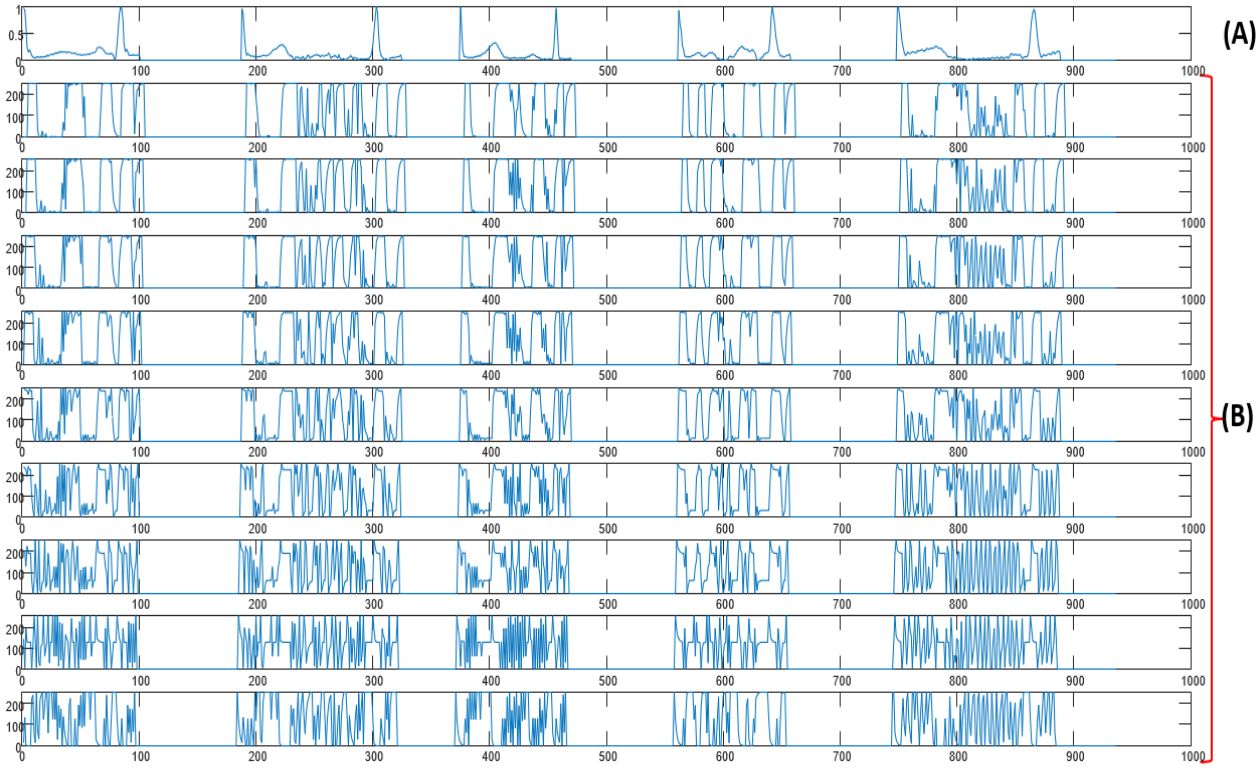

Figure 3. Implementation of the CI-1D-LBP method to a ECG sample. (A) Sample ECG signal, (B) Produced signals

Block 2: In this step, histograms of the signals generated through the implementation of the CI-1D-LBP method. The histograms corresponding to the nine different signals produced by the CI-1D-LBP method are utilized as input to the LSTM, 1D-CNN, and GRU models. The histograms of the newly generated signals also exhibit dissimilarities. Figure 4 displays the histograms corresponding to the nine different signals produced for example ECG signal, highlighting the variations between them. As demonstrated, these dissimilarities contribute to the creation of feature matrices characterizing each ECG signal instance within the dataset.

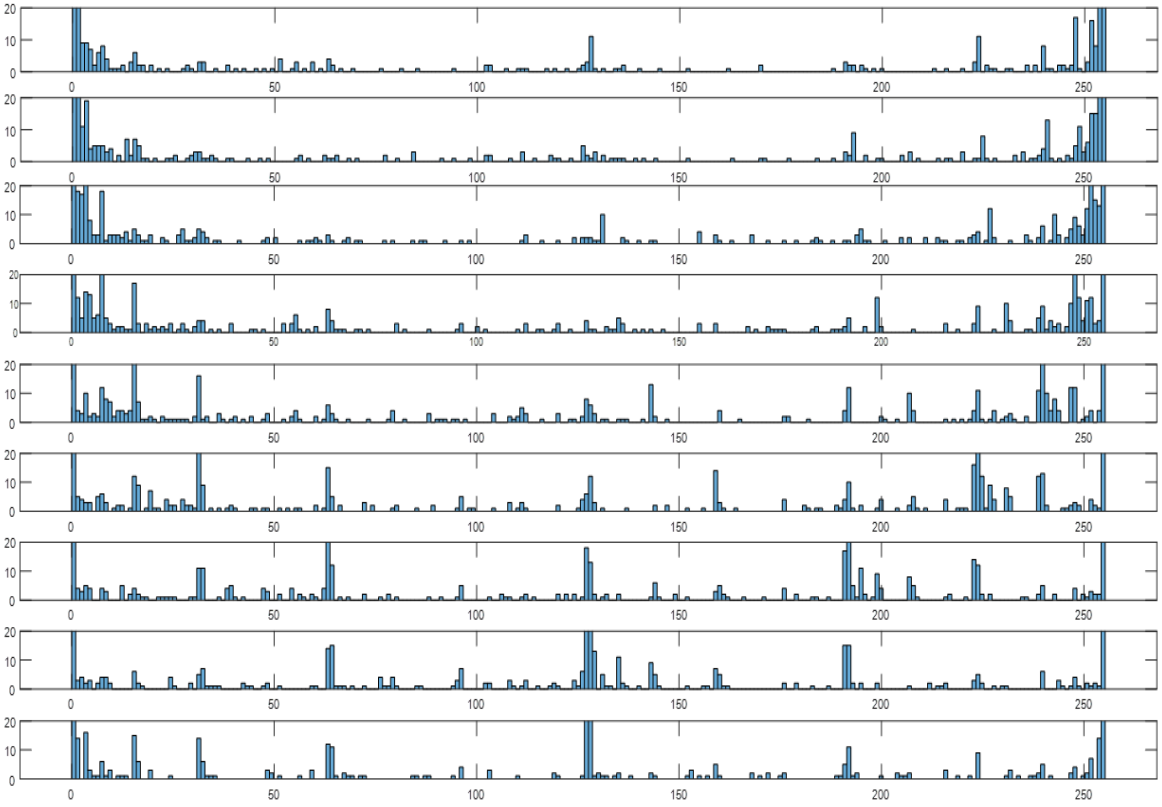

Figure 4: Histograms of the newly generated signals via CI-1D-LBP

Block 3: In this phase, the CI-1D-LBP histograms derived from the preceding stage are input into LSTM, GRU, and 1D-CNN deep learning architectures.

Block 4: This stage pertains to the decision-making process, where the classification accuracy percentage, performance parameters and confusion matrices are presented as means of evaluating the classification performance.

2.3. Center independent 1D local binary patterns (CI-1D-LBP)

The CI-1D-LBP method employs a nuanced approach, utilizing binary data derived from the comparison of each of nine discrete points within a window function applied along the ECG signal's length, relative to their neighboring counterparts. Figure 5 provides a detailed illustration of the CI-1D-LBP method, which operates by traversing the signal pointwise through a window of size WS (Window Size) = 9.

The window length of 9 was chosen in the application of the method to ensure that each selected central point on the signal could be compared with its eight neighboring points, resulting in the formation of 8-bit binary sequences. In the proposed method, the value of nine is defined as the window length(WS) within which comparisons are made. Specifically, nine points are selected within the window, and each point is compared to its eight neighboring points. This window size is critical for balancing feature richness and computational efficiency. The eight comparisons result in an 8-bit feature vector, where each bit reflects whether a particular point in the window is greater or smaller than its neighboring points.

Choosing a window length (WS) of nine ensures sufficient local detail is captured while avoiding unnecessary computational complexity. A smaller window would reduce the granularity of the features extracted, while a larger window would increase the number of comparisons, leading to higher computational costs without significant gains in feature representation. Thus, a window length of nine provides an optimal trade-off between capturing local variations in the signal and maintaining computational efficiency. These binary sequences were then used to generate histograms from the ECG samples, with values ranging between 0 and 255.At any given time, the values that enter the WS=9 window are represented as a vector P={Pc,P1,P2,P3,P4,P5,P6,P7,P8}, where Pc is the central value and P1-P8 are the surrounding values.

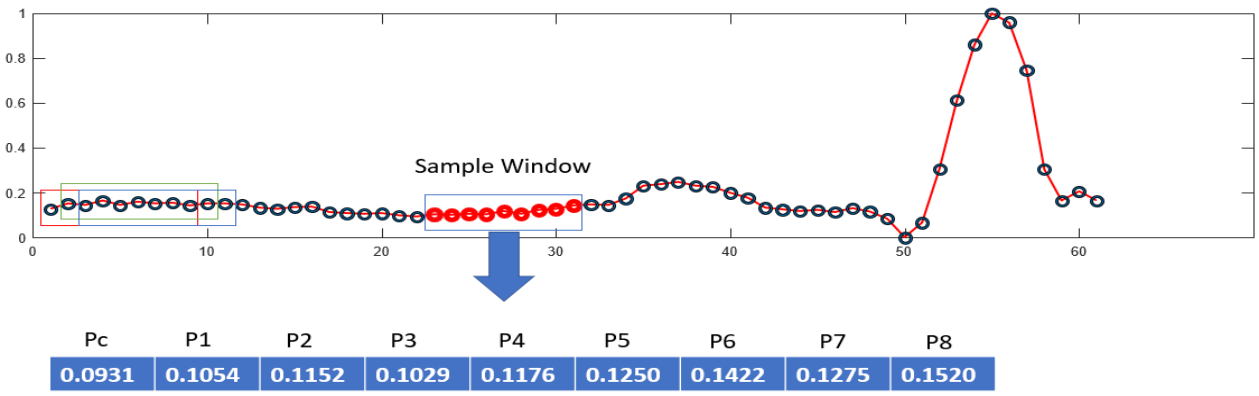

Figure 5. Application of CI-1D-LBP approach to an example ECG signal segment.

The WS window includes 9 values, one of which is Pc (Point Center), and the others are considered as neighboring P={P1,P2,P3,P4,P5,P6,P7,P8} values. The Pc value represents each value on the vector entering the WS window. As shown in Figure 6, there are 9 possible cases within the WS window. In this case, the Pc value is subjected to binary comparisons with the other values using the following equation.

$$\begin{Bmatrix} Pc > Pi \;\; 1, \;\; Pi = \{P1, P2, P3, P4, P5, P6, P7, P8\} \\ Pc \leq Pi \;\; 0, \;\; Pi = \{P1, P2, P3, P4, P5, P6, P7, P8\} \end{Bmatrix} \quad (1)$$

As shown in Figure 6, each of the nine points within the window is sequentially designated as the central point. A difference comparison is then made between the central point and the other eight points within the same window, generating an 8-bit binary value for each point. Consequently, these 8-bit sequences are used to create histograms, characterizing the signal with amplitudes ranging from 0 to 255.

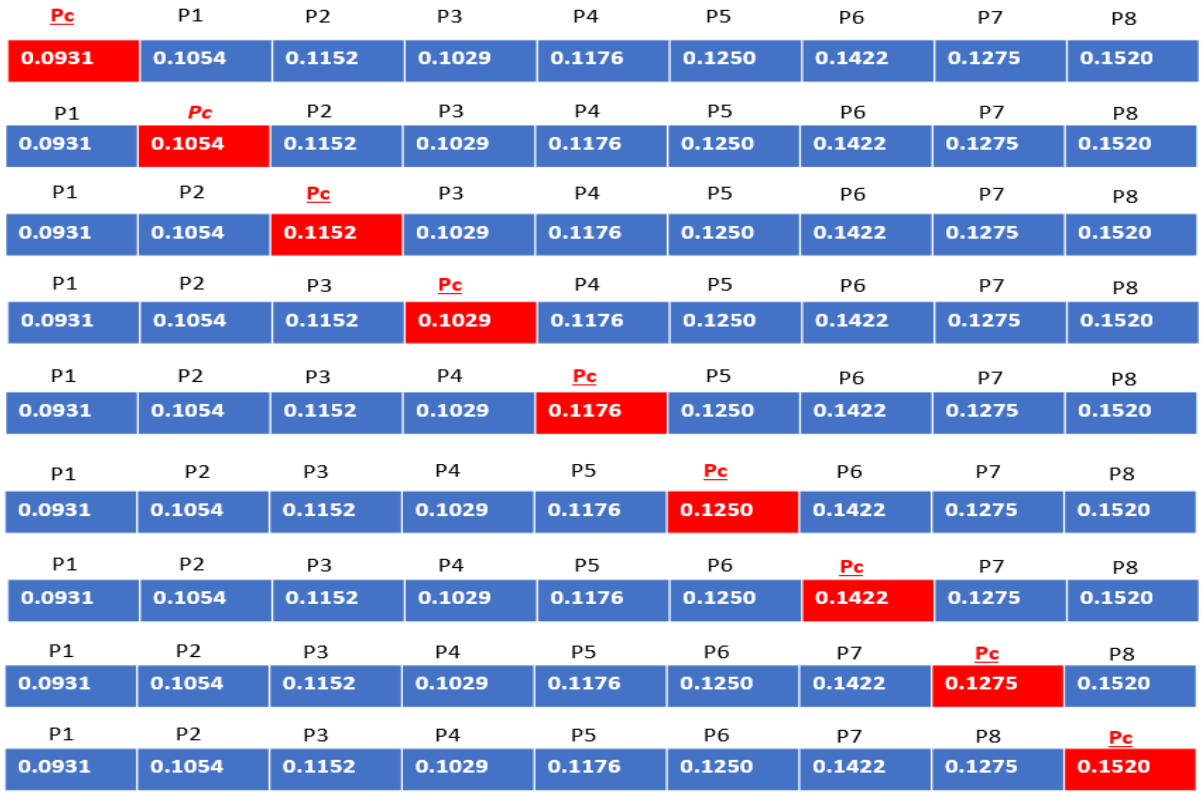

Figure 6: Computation of CI-1D-LBP value according to possible PC values

2.4. 1D-CNN

CNNs are widely employed in areas such as pattern recognition, image interpretation, medical image analysis, and natural language processing [32]. These networks can be transformed into different architectures with changes in network structures and hyperparameters depending on the problem and application [33]. In applications, there are two types of convolutional neural network models, namely 1D-CNN and 2D-CNN. Structurally, the 1D-CNN parallels the 2D-CNN network. 2D-CNNs are chiefly employed for the feature extraction and classification of two-dimensional images, whereas 1D-CNNs are specially engineered for handling the extraction and classification of one-dimensional signals, including ECG, EEG, and audio data [34]. The schematic representation of a conventional 1D-CNN network is shown Figure 7.

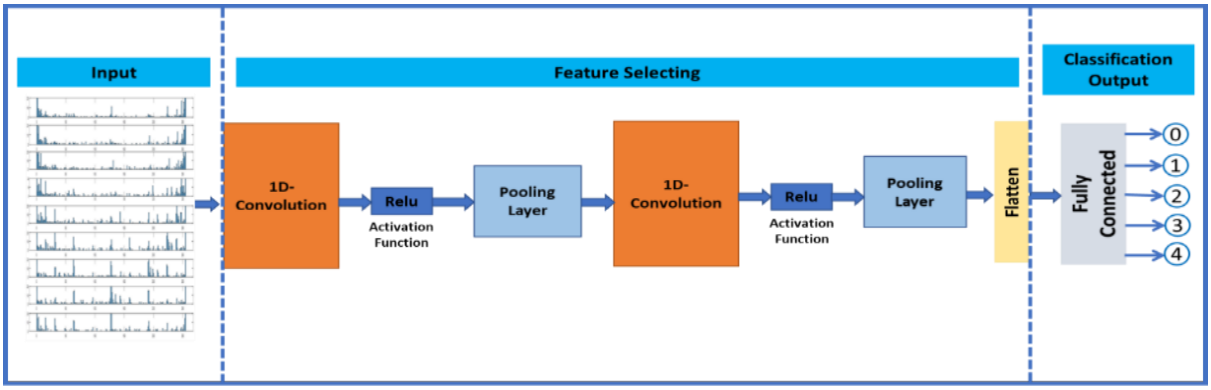

Figure 7. Block diagram structure of a 1D-CNN network

2.5. Long Short-Term Memory (LSTM)

LSTM is a unique form of Recurrent Neural Network (RNN) model specifically designed to address the RNN's shortcomings in learning long-term dependencies [35]. Employed in classification and regression applications, the LSTM architecture offers a solution to the RNN's limitations in capturing long-term dependencies.

The most significant advantage of LSTM lies in its internal sections, commonly referred to as "gates," that enable it to control the data flow throughout the network. These gates consist of four elements: the input gate, forget gate, change gate, and output gate. The gates have the unique ability to coordinate information flow both into and out of the cell, allowing for the addition or removal of information, thus endowing the cell with the capacity to remember values over designated time intervals [36]. The input gate controls when new information should enter the memory. The forget/memory gate regulates the forgetting of existing information and the remembering of new data [37]. The output section controls when the information in the cell should be used at the output of the cell [38]. The block diagram of the LSTM architecture is illustrated below.

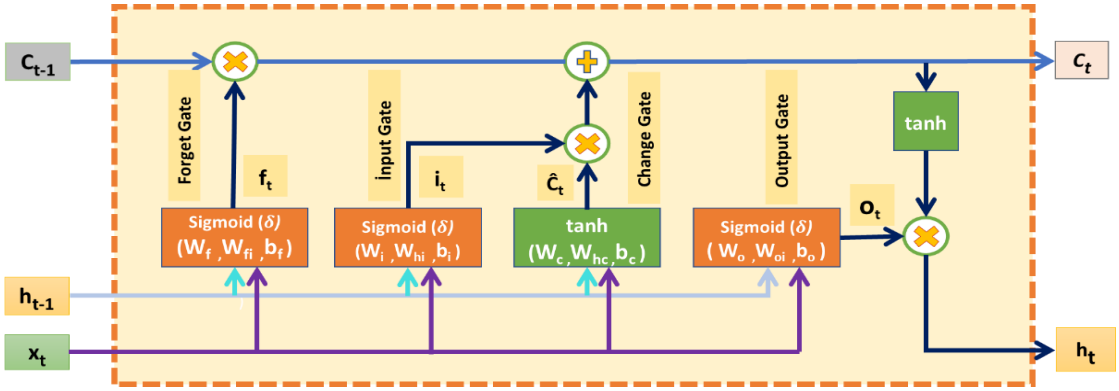

Figure 8. Representation of LSTM blocks and memory cell units.

The LSTM cell contains two states, the long-term (Ct) cell state that represents the intermediate output, and the short-term (ht) cell state. Additionally, LSTM cells contain four trainable gates: input, output, forget, and change gates [40]. These gates have the ability to control the flow of information into and out of the cell by regulating the addition or removal of information, allowing the cell to remember values at certain intervals [34]. The gates are different neural networks that decide which information will be allowed into the cell state. Moreover, during the training process, gates learn which information should be stored or forgotten in the cell state [40]. Let $x = \{x_1, x_2, \ldots, x_n\}$ be the input data at time t. The memory cell "Ct" updates the information using the input (i_t), forget (f_t) and change ($\check{C}_t$) gates. At any time "t", the corresponding gates and layers compute the following functions:

$$i_t = \sigma(W_i x_t + W_{hi} h_{t-1} + b_i) \quad (2)$$

$$f_t = \sigma(W_f x_t + W_{fi} h_{t-1} + b_f) \quad (3)$$

$$o_t = \sigma(W_o x_t + W_{oi} h_{t-1} + b_o) \quad (4)$$

$$\check{C}_t = tanh(W_c x_t + W_{hc} h_{t-1} + b_c) \quad (5)$$

$$C_t = f_t \odot C_t + i_t \odot \check{C}_t \quad (6)$$

$$h_t = o_t \odot \tanh(C_t) \quad (7)$$

Where σ and tanh are sigmoid and hyperbolic tangent activation functions. W_{hc}, W_{hi}, W_f, W_{fi}, W_o, W_{oi}, W_c, W_i are the weight matrices, b_i, b_f, b_o, b_c are the vector of threshold values. ⊙ denotes matrix or vector products. The cell state serves as a transport highway that carries relevant information and the information flow is carefully regulated by the gates. The gates are different neural networks that decide which information is allowed to enter the cell state. Additionally, during training, the gates learn which information should be stored or forgotten. The input gate is a section where a neural network generates the new memory with the help of the tanh activation function and the effect of the previous memory block. The output gate is the section where the output of the current LSTM block is produced.

The LSTM algorithm stands out with its ability to automatically extract features from time series data and learn complex nonlinear relationships [37]. Due to these properties, the LSTM algorithm is remarkable for its ability to automatically extract features from time-series data and learn complex nonlinear relationships. Therefore, the LSTM model is frequently utilized for the extraction and categorization of features from nonlinear signals, such as ECG, EMG, and EEG.

2.6. GRU (Gated Recurrent Units)

The GRU algorithm is an enhanced type of recurrent neural network (RNNs). GRU models, designed by Chu et al. (2014), are created by modifying the LSTM algorithm to mitigate the vanishing gradient problem, which impedes the learning of long-term dependencies. [38]. They use an internal memory feature and update and reset gates to store and filter information. [19]. GRU networks use gate units similar to LSTM networks to model the data flow within the unit, but without a separate memory cell, and they also have the ability to capture long-term dependencies in sequential input data or keep sequential input data in memory without deleting them for a long time, similar to LSTM networks. [41]. In the GRU model, the input and forget gates present in LSTM networks are merged into a single gate called the update gate, and this simpler design of GRU speeds up its training with fewer parameters. The GRU architecture is composed of three gates: the reset gate, the update gate, and the gate that computes the representative output vector. The reset gate governs the extent to which the previous state is to be disregarded, while the update gate determines the proportion of the previous state that should be retained, and the representative output vector gate computes the output representation. The block diagram of the GRU architecture is illustrated below.

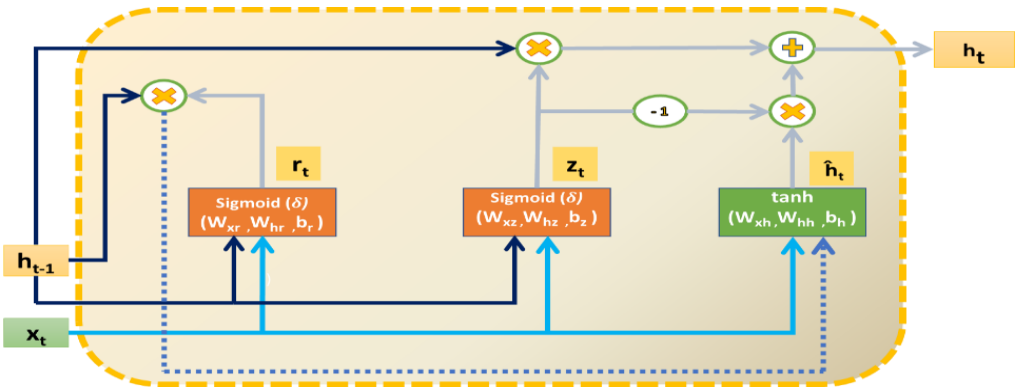

Figure 9. Structures of GRU blocks and cells

As shown in the figure, the network is fed by the current input vector x_t, while the previous layer values are expressed as h_{t-1}. W_{xr}, W_{xz}, W_{xh} ve W_{hr}, W_{hz}, W_{hh} are weight matrices. b_r, b_z, b_h are threshold value vectors. The reset gate is denoted by r_t and the update gate by z_t. In the GRU unit, instead of directly calculating the output vector h_t, a representative $\hat{h}_t$ is first calculated for it. The following equations give the mathematical expressions for the reset gate r_t, the update gate z_t, the representative output gate $\hat{h}_t$ and the output vector h_t. In the equations, the symbol $\odot$ denotes matrix or vector products.

$$r_t = \sigma(W_{xr}x_t + W_{hr}h_{t-1} + b_r) \quad (8)$$

$$z_t = \sigma(W_{xz}x_t + W_{hz}h_{t-1} + b_z) \quad (9)$$

$$\hat{h}_t = tanh(W_{xh}x_t + W_{hh}(h_{t-1} \odot r_t) + b_h) \quad (10)$$

$$h_t = z_t \odot h_{t-1} + (1 - z_t) \odot \hat{h}_t \quad (11)$$

2.7. Performance Criteria

The accuracy, precision, recall, and f-measure metrics were used to test the performance of the proposed method. The formulas for these metrics are given below.

$$Accuracy = \frac{TP+TN}{TP + TN + FP + FN} x100 \quad (12)$$

$$\text{Precision} = \frac{TP}{TP + FP} \quad (13)$$

$$\text{Recall} = \frac{TP}{TP + FN} \quad (14)$$

$$\text{F1} - \text{score} = 2x\frac{(Recall\ x\ Precision)}{\text{Recall} + \text{Precision}} \quad (15)$$

T, F, P, and N represent true, false, positive, and negative, respectively, in these equations. For example, TP represents the number of true positive signals classified, while FN represents the number of false negative signals classified.

3. Results and Discussion

In this study, the CI-1D-LBP methodology was utilized to derive unique features from ECG signals representing four distinct arrhythmia types—ventricular beats (VB), supraventricular beats (SVB), fusion beats (FB), and an indeterminate arrhythmia (UB)—as well as from ECG signals indicative of NSR in healthy subjects. This approach employs binary data derived from the comparative analysis of each of nine discrete points within a window function, applied along the length of the ECG signal, in relation to its neighboring points. Signal histograms with values ranging from 0 to 255, obtained through the aforementioned method, were constructed and utilized as inputs for LSTM, 1D-CNN, and GRU. To evaluate the effectiveness of the suggested methodology, ECG data composed of four different types of arrhythmias (VB, SVB, FB, UB) and normal sinus rhythm (NSR) were used. The hyperparameter settings for the LSTM, 1D-CNN, and GRU employed in the experiment is shown in Table 1.

Table 1 . Hyperparameter values of LSTM, 1D-CNN and GRU models

LSTM		**1D-CNN**		GRU	
Parameter	**Value**	**Parameter**	**Value**	**Parameter**	**Value**
Layers	SeguenceInput LSTM(100) fullyConnected SoftMax Classification	**Layers**	SeguenceInput convolution1dLayer reluLayer layerNormalizationLayer Convolution1dLayer reluLayer layerNormalizationLayer globalAveragePooling1dLayer fullyConnectedLayer softmaxLayer ClassificationLayer	**Layers**	sequenceInputLayer gruLayer fullyConnectedLayer softmaxLayer classificationLayer
Input size	3/256	Input size	3/256	Input size	3/256
Hidden size	100	#filters /filtersize	32-64 / 3	#filters /filtersize	32-64 / 3
Output layer size	3	Output layer size	3	Output layer size	3
Batch size / MaxEpochs	127 / 30	Batch size	127	Batch size	127
Optimizer	Adam	Optimizer	sgdm	Optimizer	rmsprop
Learning rate	0.01	MaxEpochs	70	MaxEpochs	30

The parameters given in Table 1 were fine-tuned to maximize accuracy for each deep learning model. In this study, it was established that a batch size of 127 is optimal for the LSTM, 1D-CNN, and GRU models to attain the most effective classification performance. While the MaxEpoch parameter value was set to 30 for the LSTM and GRU models, it was set to 70 for the 1D-CNN model. The accuracy rates achieved by LSTM, 1D-CNN, and GRU in the classification process for the five-labeled data set (VB-SVB-FB-UB-NSR), are shown in Table 2. The classification tasks were executed for varying training-test ratios.

Table 2. Success rates for 1D-CNN, LSTM AND GRU models

Model	Training-Test	Accuracy (%)	Recall	Precision	F1-score
CI-1D-LBP+1D CNN	70%-30%	97.17	0.953	0.952	0.952
	60%-40%	95.92	0.915	0.893	0.901
	50%-50%	95,48	0.903	0.868	0.892
CI-1D-LBP+LSTM	70%-30%	98.02	0.973	0.941	0.956
	60%-40%	96.21	0.964	0.880	0.917
	50%-50%	95.87	0.895	0.918	0.904
CI-1D-LBP+GRU	70%-30%	98.59	0.975	0.945	0.958
	60%-40%	96.25	0.933	0.904	0.918
	50%-50%	95.81	0.920	0.887	0.898

According to Table 2, high accuracies were observed for all three deep learning methods. However, in general, models with cellular network structures similar to CI-1D-LBP+LSTM and CI-1D-LBP+GRU achieved more successful results than 1D-CNNThe highest level of effectiveness was noted with the CI-1D-LBP+LSTM model as 98.02% for the 70-30 training-test set ratio. In the CI-1D-LBP-GRU model, a success rate of 98.59% was achieved again for the 70-30 training-test ratio. In the CI-1D-LBP+1D-CNN model, a success rate of 97.17% was observed for the 70-30 training-test set ratio. According to the results, the CI-1D-LBP+GRU model has shown the best performance in classifying the five-label ECG data. Confusion matrices of the most successful results of CI-1D-LBP+LSTM, CI-1D-LBP+1D-CNN, and CI-1D-LBP+GRU deep learning models in classifying the five-label ECG data are provided in Figures 10-12. The confusion matrices for both the training and test sets are presented separately. As seen from the confusion matrices, the success percentages of CI-1D-LBP+GRU for each ECG class were higher than CI-1D-LBP+LSTM and CI-1D-LBP-1D+CNN models for both training and test sets.

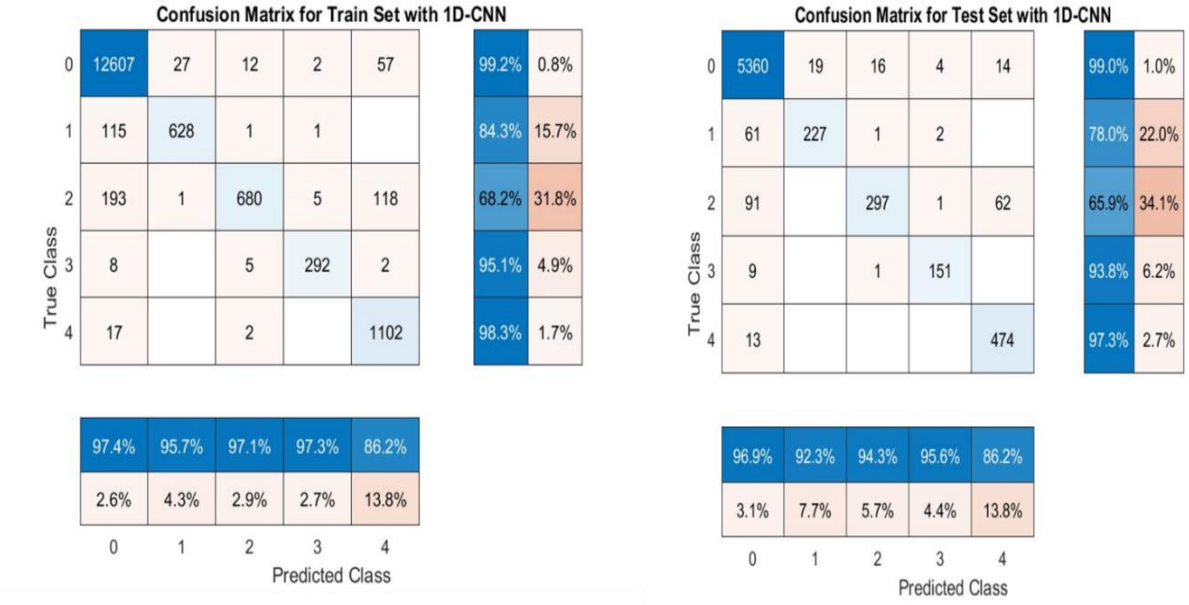

Figure 10. Confusion matrices obtained with the 1D-CNN model for the training and test sets.

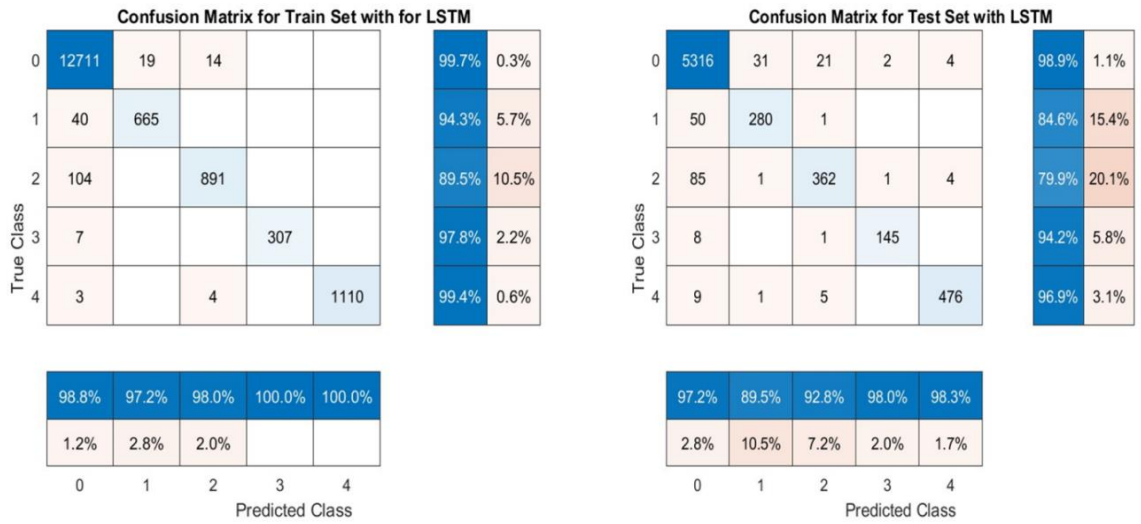

Figure 11. Confusion matrices obtained with the LSTM model for the training and test sets.

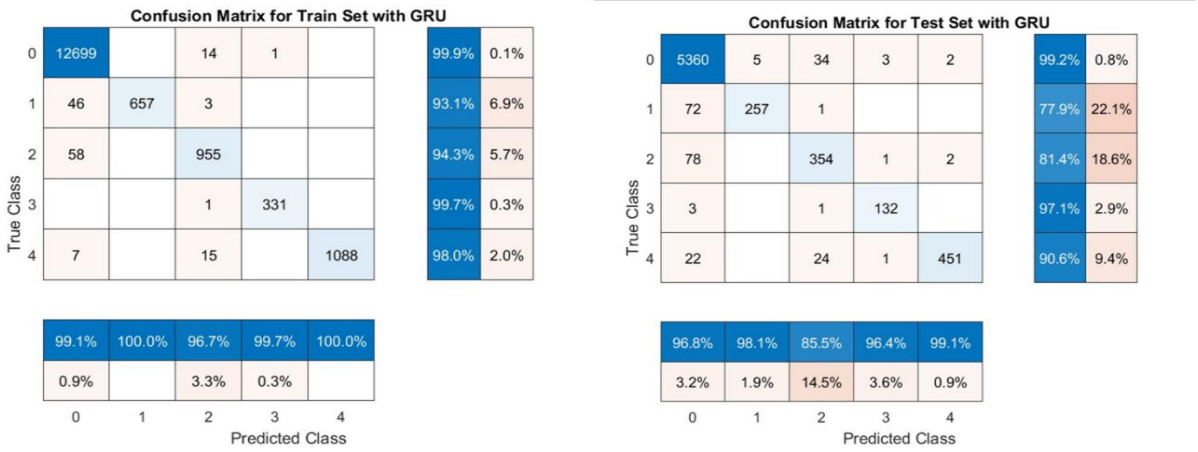

Figure 12. Confusion matrices obtained with the GRU model for the training and test sets

In the application, data sets were used in different combinations and ECG signals belonging to arrhythmia types (VB, SVB, FB, UB) consisting of four labeled data were used to classify arrhythmia types within themselves. Finally, two-labeled datasets consisting of ECG signals from each type of arrhythmia as well as normal sinus rhythm (NSR) were classified separately (i.e., VB-NSR, SVB-NSR, FB-NSR, and UB-NSR). The achieved performance results are presented in Table 3.

Table 3. Classification success (accuracy) rates for different dataset combinations

Datasets	CI-1D LBP+LSTM	CI-1D-LBP-1D+CNN	CI-1D-LBP+GRU
VB-SVB-FB-UB	98.70	97.81	99.08
NSR-VB	99.12	98.23	99.87
NSR-SVB	99.20	98.19	100
NSR-FB	99.47	98.48	99.71
NSR-UB	99.66	98.32	100

It can be observed that the CI-1D-LBP+GRU and CI-1D-LBP+LSTM models outperform the CI-1D-LBP+1D-CNN model in terms of accuracy. Moreover, the CI-1D-LBP+GRU model exhibits the best performance in all two-labeled and four-labeled ECG dataset classifications. The classification performance of ECG data with different signal lengths was tested thanks to the preprocessing steps applied to the dataset. Thus, the effect of ECG data length on classification performance was observed. Upon examination of the results, it can be observed that the classification performance and accuracy of

the proposed models increases as the length of the signal increases. Table 4 presents the classification accuracy rates for the five labeled datasets consisting of NSR and four different arrhythmia types (NSR, VB, SVB, FB, UB) with varying signal lengths.

Table 4. Performance rates (%) according to different signal lengths.

Signal length(Samples)	CI-1D-LBP-LSTM	CI-1D-LBP-1D CNN	CI-1D-LBP-GRU
187	91.20	89.10	91.89
374	92.11	91.32	92.81
561	94.05	93.14	94.76
748	95.24	94.18	95.83
935	96.31	95.91	96.81
1122	97.04	96.33	97.60
1309	98.02	97.17	98.59

The following Table 5 presents the accuracy percentages of the deep learning methods used in previous studies on arrhythmia classification in the literature and the accuracy percentages of this study. Upon analysis of the results, it has been observed that proposed CI-1D-LBP+GRU method, which yielded better results compared to CI-1D-LBP+LSTM and CI-1D-LBP+1D-CNN methods in this study, also outperformed the deep learning methods used in the literature.

Table 5. Evaluating the CI-1D-LBP+GRU in relation to findings from previous research.

Referance	Datasets	Methods	Number of Labeled class in ECG dataset	Performance (Accuracy)(%)
Zheng et al	Three Types ARR and NSR	Singular Value Decomposition (SVD)-CNN-SVM	4	96-97
Murawwat et al	Two types of arrhythmias: Tachycardia and Bradycardia	Multivariate Empirical Mode Decomposition (MEMD)-ANN	3	89.8
Li et al.	NSR and CHF	Distance distribution matrics + CNN	2	81.85
Sharma et al	Four Type ARR, NSR	Fourier-Bessel expansion + LSTM	5	90.07
Çınar and Tuncer	Congestive Heart Failure (CHF), ARR, NSR	Hybrid Alexnet-SVM	3	96.77
Kaouter et al.	Congestive Heart Failure (CHF), ARR, NSR	2D-CNN	3	93.75
Acharya et al	Four Type ARR and NSR	9-layer deep convolutional neural network (CNN)	5	93.50
Kumari et al.	Four Type ARR and NSR	DWT + SVM	5	95.92
This Study	**Four Type ARR and NSR**	**CI-1D-LBP+GRU**	**5**	**98.59**

The Table 5 presents a comparative analysis of various ECG classification methods, highlighting the number of labeled classes and their corresponding performance in terms of accuracy. Methods such as SVD-CNN-SVM, Hybrid AlexNet-SVM, and DWT-SVM show strong results across different datasets, with accuracies ranging from 89.8% to 96.77%. However, the proposed CI-1D-LBP + GRU method demonstrates superior performance, achieving the highest accuracy among the compared approaches. By leveraging the strengths of Local Binary Patterns (LBP) for feature extraction and GRU for modeling temporal dependencies, this study's method offers a more robust and precise classification framework, effectively surpassing traditional and deep learning-based methods.

4. Conclusion

ECGs are extensively utilized for the prompt and precise examination of cardiovascular conditions. In this study, the CI-1D-LBP methodology was introduced for deriving features from ECG signals. When applied to an ECG signal, this method produces 9 different signals. The histograms of these signals, which have values ranging from 0 to 255, were used as inputs to 1D-CNN, LSTM, and GRU deep learning methods.

Computer-assisted diagnostic systems depend on the efficacy of features extracted from ECG signals to ensure accurate heart disease diagnosis. The LSTM, 1D-CNN, and GRU deep learning architectures have been identified as particularly effective classification models, owing to their proven success in analyzing time series data. The ability of deep learning methods to perform feature extraction and classification of data within a single model structure is particularly useful for analyzing high-dimensional, non-stationary data such as ECG.

The CI-1D-LBP+GRU method applied in this study has superior features due to its capacity to model extended temporal dependencies in time series data and retain data in memory for a long time without discarding, which is especially advantageous for the analysis of high-dimensional data such as ECG. Moreover, the CI-1D-LBP+GRU methodology exhibits enhanced capabilities due to its proficiency in identifying and maintaining prolonged temporal dependencies in time series data and preserving data within memory for extended periods without degradation. This attribute proves especially beneficial for the analysis of non-stationary and high-dimensional datasets, such as ECG signals.

The comparison of various ECG classification methods highlights the unique advantages and originality of the proposed CI-1D-LBP+GRU approach in this study. Unlike previous works that rely on conventional feature extraction techniques or deep learning architectures, this method introduces a novel combination of 1D Local Binary Patterns (LBP) for capturing intricate local signal variations, paired with GRU for effectively modeling temporal dependencies. This dual approach allows for a more refined feature representation, enabling superior classification performance across different types of arrhythmias. While several established methods have shown promising results, the integration of LBP with recurrent neural networks offers a fresh perspective that addresses both the spatial and temporal complexities inherent in ECG signals, demonstrating the potential for more accurate and reliable diagnosis in practical applications.

In addition, the CI-1D-LBP+GRU method has lower cellular network complexity compared to the CI-1D-LBP+LSTM model, which has a similar network structure. These superior features of the CI-1D-LBP+GRU have also been demonstrated in the application results. The CI-1D-LBP+GRU method outperformed CI-1D-LBP+LSTM and CI-1D-LBP-1D+CNN in the classification of the five-labeled data set (VB-SVB-FB-UB-NSR), and an accuracy rate of 98.59% was achieved.

Building on the success of the CI-1D-LBP+GRU methodology, future research could explore its application to larger and more diverse ECG datasets to further validate its robustness across different populations and conditions. Additionally, integrating the method with real-time monitoring systems could facilitate early detection of arrhythmias in clinical settings. Enhancing the model by incorporating advanced techniques such as attention mechanisms or hybrid deep learning frameworks could also improve interpretability and performance. Furthermore, expanding this approach to detect and classify additional cardiac anomalies would broaden its potential impact in the field of healthcare diagnostics.

Author Contribution Statement

Conceptualization: HT
Method: YK
Manuscript writing reviewing editing: YK, HT
Supervision: HT

Conflict of Interest

The authors declare no competing interest.

Statement of Research and Publication Ethics

The study is complied with research and publication ethics.

References

[1] H. E. Fürniss and B. Stiller, "Arrhythmic risk during pregnancy in patients with congenital heart disease.," *Herzschrittmacherther Elektrophysiol*, vol. 32, no. 2, pp. 174–179, 2021.

[2] F. A. Elhaj, N. Salim, A. R. Harris, T. T. Swee, and T. Ahmed, "Arrhythmia recognition and classification using combined linear and nonlinear features of ECG signals," *Comput Methods Programs Biomed*, vol. 127, pp. 52–63, 2016.

[3] H. V Huikuri, A. Castellanos, and R. J. Myerburg, "Sudden death due to cardiac arrhythmias," *New England Journal of Medicine*, vol. 345, no. 20, pp. 1473–1482, 2001.

[4] X. Xu, S. Jeong, and J. Li, "Interpretation of electrocardiogram (ECG) rhythm by combined CNN and BiLSTM," *Ieee Access*, vol. 8, pp. 125380–125388, 2020.

[5] F. Miao, B. Zhou, Z. Liu, B. Wen, Y. Li, and M. Tang, "Using noninvasive adjusted pulse transit time for tracking beat-to-beat systolic blood pressure during ventricular arrhythmia," *Hypertension Research*, vol. 45, no. 3, pp. 424–435, 2022.

[6] M. J. Curtis *et al.*, "The Lambeth Conventions (II): guidelines for the study of animal and human ventricular and supraventricular arrhythmias," *Pharmacol Ther*, vol. 139, no. 2, pp. 213–248, 2013.

[7] M. A. Arias, M. Pachón, and C. Martín-Sierra, "A regular wide QRS complex tachycardia with fusion beats?," *J Arrhythm*, vol. 36, no. 6, p. 1100, 2020.

[8] S. Ayub and J. P. Saini, "ECG classification and abnormality detection using cascade forward neural network," *International Journal of Engineering, Science and Technology*, vol. 3, no. 3, 2011.

[9] A. Çalışkan, "A new ensemble approach for congestive heart failure and arrhythmia classification using shifted one-dimensional local binary patterns with long short-term memory," *Comput J*, vol. 65, no. 9, pp. 2535–2546, 2022.

[10] S. Sahoo, M. Dash, S. Behera, and S. Sabut, "Machine learning approach to detect cardiac arrhythmias in ECG signals: A survey," *Irbm*, vol. 41, no. 4, pp. 185–194, 2020.

[11] Y. Kaya, F. Kuncan, and R. Tekin, "A new approach for congestive heart failure and arrhythmia classification using angle transformation with LSTM," *Arab J Sci Eng*, vol. 47, no. 8, pp. 10497–10513, 2022.

[12] A. S. Eltrass, M. B. Tayel, and A. I. Ammar, "A new automated CNN deep learning approach for identification of ECG congestive heart failure and arrhythmia using constant-Q non-stationary Gabor transform," *Biomed Signal Process Control*, vol. 65, p. 102326, 2021.

[13] D. Thanapatay, C. Suwansaroj, and C. Thanawattano, "ECG beat classification method for ECG printout with Principle Components Analysis and Support Vector Machines," in *2010 International Conference on Electronics and Information Engineering*, IEEE, 2010, pp. V1-72.

[14] S. Karpagachelvi, M. Arthanari, and M. Sivakumar, "Classification of electrocardiogram signals with support vector machines and extreme learning machine," *Neural Comput Appl*, vol. 21, pp. 1331–1339, 2012.

[15] M. Vijayavanan, V. Rathikarani, and P. Dhanalakshmi, "Automatic classification of ECG signal for heart disease diagnosis using morphological features," *International Journal of Computer Science & Engineering Technology*, vol. 5, no. 4, pp. 449–455, 2014.

[16] S. Hadiyoso and A. Rizal, "Electrocardiogram signal classification using higher-order complexity of hjorth descriptor," *Adv Sci Lett*, vol. 23, no. 5, pp. 3972–3974, 2017.

[17] J. A. Gutiérrez-Gnecchi *et al.*, "DSP-based arrhythmia classification using wavelet transform and probabilistic neural network," *Biomed Signal Process Control*, vol. 32, pp. 44–56, 2017.

[18] Z. Wu *et al.*, "A novel features learning method for ECG arrhythmias using deep belief networks," in *2016 6th International conference on digital home (ICDH)*, IEEE, 2016, pp. 192–196.

[19] H. M. Lynn, S. B. Pan, and P. Kim, "A deep bidirectional GRU network model for biometric electrocardiogram classification based on recurrent neural networks," *IEEE Access*, vol. 7, pp. 145395–145405, 2019.

[20] U. R. Acharya *et al.*, "Deep convolutional neural network for the automated diagnosis of congestive heart failure using ECG signals," *Applied Intelligence*, vol. 49, pp. 16–27, 2019.

[21] S. Han, W. Lee, H. Eom, J. Kim, and C. Park, "Detection of arrhythmia using 1D convolution neural network with LSTM model," *IEIE Transactions on Smart Processing & Computing*, vol. 9, no. 4, pp. 261–265, 2020.

[22] A. Darmawahyuni, S. Nurmaini, M. Yuwandini, M. N. Rachmatullah, F. Firdaus, and B. Tutuko, "Congestive heart failure waveform classification based on short time-step analysis with recurrent network," *Inform Med Unlocked*, vol. 21, p. 100441, 2020.

[23] L. Zheng, Z. Wang, J. Liang, S. Luo, and S. Tian, "Effective compression and classification of ECG arrhythmia by singular value decomposition," *Biomedical Engineering Advances*, vol. 2, p. 100013, 2021.

[24] A. Çınar and S. A. Tuncer, "Classification of normal sinus rhythm, abnormal arrhythmia and congestive heart failure ECG signals using LSTM and hybrid CNN-SVM deep neural networks," *Comput Methods Biomech Biomed Engin*, vol. 24, no. 2, pp. 203–214, 2021.

[25] S. C. Mohonta, M. A. Motin, and D. K. Kumar, "Electrocardiogram based arrhythmia classification using wavelet transform with deep learning model," *Sens Biosensing Res*, vol. 37, p. 100502, 2022.

[26] P. Madan, V. Singh, D. P. Singh, M. Diwakar, B. Pant, and A. Kishor, "A hybrid deep learning approach for ECG-based arrhythmia classification," Bioengineering, vol. 9, no. 4, p. 152, 2022.

[27] E. B. Panganiban, A. C. Paglinawan, W. Y. Chung, and G. L. S. Paa, "ECG diagnostic support system (EDSS): A deep learning neural network based classification system for detecting ECG abnormal rhythms from a low-powered wearable biosensors," Sensing and Bio-Sensing Research, vol. 31, p. 100398, 2021.

[28] M. Salem, S. Taheri, and J. Yuan, "ECG arrhythmia classification using transfer learning from 2-dimensional deep CNN features," in 2018 IEEE Biomedical Circuits and Systems Conference (BioCAS), 2018, pp. 1–4.

[29] J. Rahul and L. D. Sharma, "Automatic cardiac arrhythmia classification based on hybrid 1-D CNN and Bi-LSTM model," *Biocybern Biomed Eng*, vol. 42, no. 1, pp. 312–324, 2022.

[30] G. B. Moody and R. G. Mark, "The impact of the MIT-BIH arrhythmia database," *IEEE engineering in medicine and biology magazine*, vol. 20, no. 3, pp. 45–50, 2001.

[31] A. L. Goldberger *et al.*, "PhysioBank, PhysioToolkit, and PhysioNet: components of a new research resource for complex physiologic signals," *Circulation*, vol. 101, no. 23, pp. e215–e220, 2000.

[32] L. Eren, T. Ince, and S. Kiranyaz, "A generic intelligent bearing fault diagnosis system using compact adaptive 1D CNN classifier," *J Signal Process Syst*, vol. 91, pp. 179–189, 2019.

[33] A. Vijayvargiya, R. Kumar, and N. Dey, "Voting-based 1D CNN model for human lower limb activity recognition using sEMG signal," *Phys Eng Sci Med*, vol. 44, pp. 1297–1309, 2021.

[34] T.-H. Hsieh and J.-F. Kiang, "Comparison of CNN algorithms on hyperspectral image classification in agricultural lands," *Sensors*, vol. 20, no. 6, p. 1734, 2020.

[35] S. Hochreiter and J. Schmidhuber, "Long short-term memory," *Neural Comput*, vol. 9, no. 8, pp. 1735–1780, 1997.

[36] X. Hu, S. Yuan, F. Xu, Y. Leng, K. Yuan, and Q. Yuan, "Scalp EEG classification using deep Bi-LSTM network for seizure detection," *Comput Biol Med*, vol. 124, p. 103919, 2020.

[37] F. Landi, L. Baraldi, M. Cornia, and R. Cucchiara, "Working memory connections for LSTM," *Neural Networks*, vol. 144, pp. 334–341, 2021.

[38] K. Khalil, O. Eldash, A. Kumar, and M. Bayoumi, "Economic LSTM approach for recurrent neural networks," *IEEE Transactions on Circuits and Systems II: Express Briefs*, vol. 66, no. 11, pp. 1885–1889, 2019.

[39] K. Smagulova and A. P. James, "A survey on LSTM memristive neural network architectures and applications," *Eur Phys J Spec Top*, vol. 228, no. 10, pp. 2313–2324, 2019.

[40] K. Cho *et al.*, "Learning phrase representations using RNN encoder-decoder for statistical machine translation," *arXiv preprint arXiv:1406.1078*, 2014.

[41] K. A. Althelaya, E.-S. M. El-Alfy, and S. Mohammed, "Stock market forecast using multivariate analysis with bidirectional and stacked (LSTM, GRU)," in *2018 21st Saudi Computer Society National Computer Conference (NCC)*, IEEE, 2018, pp. 1–7.